Real-time State Estimation on Micro-grids

Ying Hu, Anthony Kuh, Aleksandar Kavcic
Dept. of Electrical Engineering
University of Hawaii at Manoa
Honolulu, HI 96822
Email: (huying,kuh,kavcic)@hawaii.edu

Dora Nakafuji
Hawaiian Electric Company, Inc.
PO Box 2750
Honolulu, HI 96840
Email: dora.nakafuji@heco.com

Abstract—This paper presents a new probabilistic approach of the real-time state estimation on the micro-grid. The grid is modeled as a factor graph which can characterize the linear correlations among the state variables. The factor functions are defined for both the circuit elements and the renewable energy generation. With the stochastic model, the linear state estimator conducts the Belief Propagation algorithm on the factor graph utilizing real-time measurements from the smart metering devices. The result of the statistical inference presents the optimal estimates of the system state. The new algorithm can work with sparse measurements by delivering the optimal statistical estimates rather than the solutions. In addition, the proposed graphical model can integrate new models for solar/wind correlation that will help with the integration study of renewable energy. Our state-of-art approach provides a robust foundation for the smart grid design and renewable integration applications.

I. INTRODUCTION

State estimation can provide necessary monitoring of the grid for many system optimization applications [1]. First, with the estimates of bus voltages, load tap changer (LTC) or line voltage regulator can adjust the voltage level (i.e. dynamic voltage optimization and thus control the power flow). Second, with real-time voltage and current estimates, the buses or branches that exceed their electrical limits can be identified. The corresponding faults can be predicted or eliminated. Third, by knowing the real-time power output from the renewable energy generation (REG), we can study their effect on circuit stability and other integration issues. Contingency analysis can be performed on the grid to test the maximum amount of renewable energy integration that the grid can accommodate.

State estimation has been mainly applied on the transmission system. Every few seconds the measurements are telemetered to the energy control center (e.g. SCADA). Bad data is filtered by taking advantage of data redundancy. Recently distribution system state estimation (DSE) [2][3] is drawing attention for utility planning purpose since the scale of grid monitoring, power dispatch and load shedding ability needs to be redefined. The current focus of DSE approaches may cover the part of the power system from transmission substation to feeder circuit transformer. DSE provides robust estimation of the operating state of the distribution system.

Despite of the promising applications, very little analysis has been made on the individual feeder circuit estimating the customer load characteristics. One reason for this lack of study is that there is hardly any real-time load measurements for individual customers, such as a household or a building. As a result, many utilities do not place real-time intelligent supervision and control on the circuits beyond the distribution substation. However, this situation is changing as we are experiencing a transformation of the power grid. The future smart grid [4] will bring advanced metering and management to individual customers and enable two-way flow of information from the customers to the control centers. The real-time operating state of the feeder circuits will facilitate the substation automation and load management.

Effective monitoring and control of the grid require real-time analysis tool that can estimate the system state and also predict the response of the system to changing load and weather conditions [5]. On the one hand, power system analysis requires dynamic network topology and real-time measurements. As more smart metering devices are being deployed on the grid, power system analysis is provided with data of higher accuracy and resolution. However, the wide deployment of the metering devices is limited by their high price and consequential communication burden. When metering devices are only installed at key locations on the grid, state estimation can serve as an useful technique to "fill-in" the missing points as well as "smooth-out" the noisy measurements. The estimation result reflects the true state of the circuit parameters (i.e. bus voltages, real and reactive power flow on the branches).

On the other hand, various issues such as circuit stability and load balancing problems arise due to the increasing penetration of renewable energy generation. By viewing the REG simply as negative load, current utilities are often blind to the exact behavior of the REG and their effect on the circuit parameters. Instead, the micro-grid that we are studying can realize the emerging potential of distributed renewable generation. Micro-grid is defined as a subsystem of the power grid that incorporates both associated loads and distributed generation [6]. It includes the downstream circuits of the distribution substation. The methodology deployed in the micro-grid state estimation can be later applied in the sub-transmission and distribution system state estimation that addresses the renewable energy integration. The micro-grid is also featured with smart metering devices that enables two-way flow of real-time measurements, remote metering configuration and load control etc. In a word, we seek a new state estimation approach to address the data

assessment on the micro-grid and inform the renewable energy integration.

In order to estimate the states of the micro-grid, we formulate the system as a stochastic model with graphical representation and conduct the statistical inference using an efficient signal processing algorithm. Upon convergence we can find the posterior mean of every variable, which constructs the optimal estimates of all the node behaviors. Section V introduces this approach and briefly discusses the main algorithm. Section II presents in detail the mathematical formulation of the power grid. Section III and IV further discuss the modeling method of state variables and factor functions. Section VI lists a few simulation results. Section VII concludes the discussion and points out possible future research.

II. Modeling

For simplicity reason, we mainly focus on the steady state case and the balanced three phase system. Hence per phase analysis should be sufficient for estimation purpose. Later on the study can be further extended to the unbalanced three phase distribution system. Given the one-line diagram of a distribution system, the first step is to transform it into a bus/branch model through topology processors.

The topology processor should be able to track the changing status of switches and breakers. One way of implementing the tracking mode is to verify zero flows in open switching devices and zero voltage differences across closed switching devices [1]. When there are failures caused by natural disasters, the topology processor should also be able to track the circuit changes. In conclusion, the bus/branch model provided by the topology processor is assumed to correctly represent the system.

All the buses and branches should be labeled by the topology processor. The following are a few notes regarding to the bus/branch model:

1) Every bus is labeled with a unique number.
2) The number of a branch is determined by its upstream and downstream buses.
3) Every load and REG is associated with a bus and is connected to the system through a separate branch.

Fig. 1 shows the typical bus/branch model of a simplified micro-grid. The substation is connected to a feeder circuit through a step down transformer which transforms the voltage level from $46\ KV$ to $12\ KV$. The individual customer load $(B1, B2, B3, B4)$ is denoted by a square and the REG is denoted by a star.

A factor graph can be formed from the bus-branch model. Every variable node characterizes the probability distribution of either the bus voltage phasor or the branch current phasor in the bus/branch model. In this way voltage and current are modeled separately and their correlations can be captured in the corresponding factor nodes. Power flow can be derived in the post-calculation.

Fig. 2 is the corresponding factor graph for Figure 1. Here we use the "Normal factor graph" [7] which captures two-way
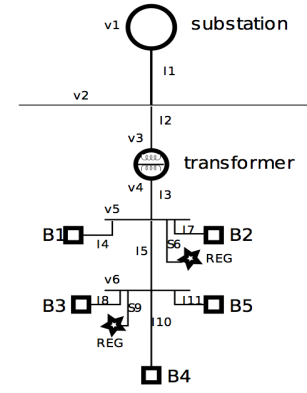

Fig. 1.   The bus/branch model of a typical micro-grid

flow of messages. The factor graph comprises two layers, i.e. behavior layer and observation layer.

In the behavior layer a circle denotes a variable node which corresponds to the bus voltage or branch current in Fig. 1 with the same number. The square denotes the correlation function of the connected variables. The meanings of different factors are listed in the following.
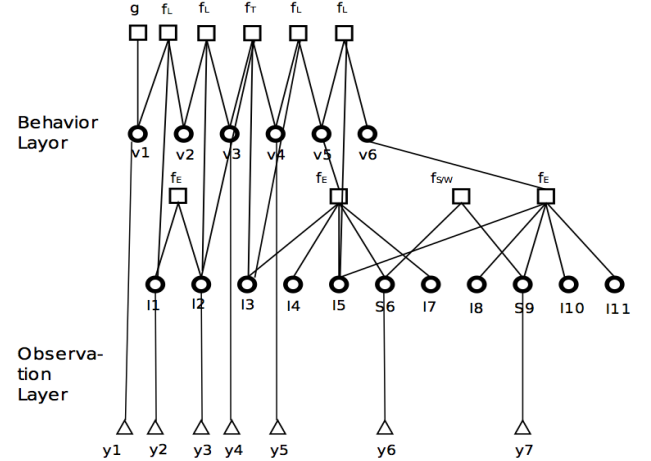

Fig. 2.   The factor graph of Fig. 1

1) g is the factor function which describes the dependence of the variable on the parameters of the voltage controlled bus.
2) f_E represents the electrical relationship at the bus.
3) f_L and f_T are the factor functions for the distribution line and the transformer respectively.
4) f_S and f_W are the solar and wind factor functions due to the spatial and temporary correlations among the REG.

The observation layer includes the nodes (denoted by triangle) which represent the observations of the variables. We apply the additive white Gaussian noise (AWGN) model for the noisy observations. At time t an observation y_t of the true state x_t is made according to

$$y_t = x_t + z_t \qquad (1)$$

where z_t is the observation noise, $z_t \sim N(0, R)$. The variance R of the noise term can be used to address the reliability of the observation (i.e. the weight of the measurements on the state estimates). The observations from smart metering devices tend to provide data with high accuracy and the noise mainly comes from the communication channel. Measurements from SCADA and the generated pseudo-measurements may introduce more noise to the true observations. Thus their corresponding R should be higher. There are empirical studies discussing the weighting factor (e.g. [8]). Currently the weighting matrix is not included in our study.

III. State Variables

Since we adopt the stochastic approach for the micro-grid state estimation, the system states are the random variables that characterize the probabilistic distribution of the corresponding electrical parameters. The probabilistic approach can provide robust estimation of the system states by calculating both the first and second order statistics. The electrical parameters in the power system state estimation usually include bus voltage, branch current, real and reactive power flow. In order to adopt the linear state estimator, the bus voltage phasor and branch current phasor are selected here to be the state variables. In the complex domain, the voltage and current can be expressed as (2).

$$\begin{cases} V_i = V_{i,real} + jV_{i,imag} \\ I_i = I_{i,real} + jI_{i,imag} \end{cases} \quad (2)$$

Every variable can be represented by a $2 * 1$ vector as in (3).

$$\begin{cases} V_i = \begin{pmatrix} V_{i,real} \\ V_{i,imag} \end{pmatrix} \\ I_i = \begin{pmatrix} I_{i,real} \\ I_{i,imag} \end{pmatrix} \end{cases} \quad (3)$$

The available measurements for the REG are usually the injected real and reactive power. So for the branches that are associated with the REG, the state variables can be defined as the upstream bus voltage and complex power flow in the branch. The complex power flow and its vector representation are shown in (4) and (5).

$$S_i = P + jQ \quad (4)$$

$$S_i = \begin{pmatrix} P \\ Q \end{pmatrix} \quad (5)$$

Since the complex power from the REG is defined as a state variable, the correlation among neighboring REG can be clearly represented by the factor function $f_{S/W}$. As shown in Fig. 2, the factor node $f_{S/W}$ is connected with $S6$ and $S9$ which address the complex power flow at conductor 6 and 9 respectively.

When the state variables are defined as phasor voltage and current, intuitively the factor functions are linear and a linear state estimator should suffice the estimation purpose. However

when the circuit equation is involved with complex power, the corresponding correlation functions are nonlinear. These correlation functions need to be linearized before applying the linear state estimation approach. For computation purpose, after linearization all the factor functions can be represented by three linear building blocks: addition, equation and multiplication by constants, as shown in Fig. 3 [9]. The modeling method of all the correlation functions using these linear blocks will be discussed in Section. IV.

(a) $\delta(X - Y)\delta(X - Z)$ (b) $\delta(X + Y - Z)$
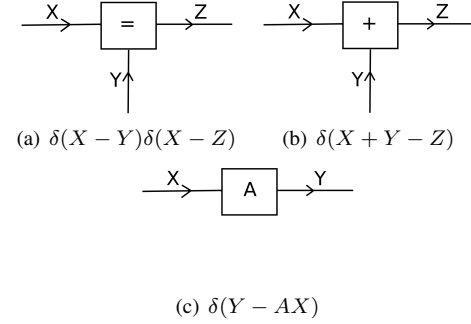
(c) $\delta(Y - AX)$

Fig. 3. Three factors representing linear building blocks

The micro-grid state estimation computes the means and variances of the state variables in a fixed time interval or when new observations are available. Many studies assume the probability distribution of the electrical parameters are Gaussian. If the state variables X and the observations Y are jointly Gaussian, the entire conditional distribution of X given $Y = y$ can be determined from the mean and variance estimates.

As the analysis gets closer to the customer end, the distribution of the state variables at different buses display a number of variations and may not match any specific distribution. However it is reasonable to approximate the load pdf using some well known pdf, such as Gaussian mixtures. Reference [10] justifies this approach by conducting several simulation studies and further reduce the components of the mixtures. The components merging results in a single Gaussian pdf which provides a better approximation of the original pdf than the approach without mixture reduction.

Study needs to be conducted on the pdf of the REG. The transform from the solar or wind resource to the REG follows the power production curve of the solar panel or wind turbine. The typical power production curve tends to be linear for certain regions (i.e. the power output is proportional to the renewable resource). For simplicity reason our study will focus on the linear region so that different panel specifications can be avoided. With the slope of the linear region, the correlation of solar irradiance or wind speed among neighboring sites can determine the correlation of the REG.

In order to test the probability distribution of the solar irradiance, we collect the mid-day solar irradiance data from the solar sensors at Castle High School on the island of Oahu, Hawaii from June 2009 to September 2009. The top sub-figure in Fig. 4 shows the pdf of the statistical data. The general

shape of the plot is close to a Gaussian distribution. The bottom sub-figure is the normal probability plot of the data. If the data are normal the plot will be linear and follow the line shown in the figure. From the figure we can tell that the normplot closely follows the red line, which means the assumption of the Gaussian distribution for the REG can be justified. If the weather condition is taken into account (e.g. the cloud movement or seasonal weather change), the Gaussian assumption may be inaccurate. Section IV will discuss more about the switch between successive Markov states, which can catch the non-linearity of Gaussian process.
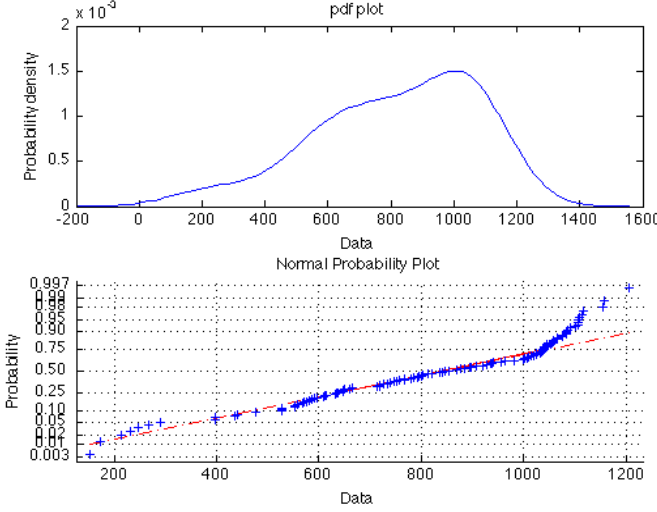

Fig. 4.   pdf and normplot of solar irradiance

IV. Correlation Functions

In Section II we briefly introduced different kinds of factor functions. In this section, every factor function is defined with a set of equations representing different correlations.

The bus that is connected to the substation can be viewed as voltage controlled bus. It usually comes with voltage and real power specification: V_g and P_g. So the factor g can be defined as (6):

$$\begin{cases} V_1 = V_g \\ Re\{V_1 I_1^*\} = P_g \end{cases} \tag{6}$$

The factor f_E describes the electrical relationship at the bus. In Fig. 1, the f_E function at bus 5 can be defined as (7):

$$I_3 = I_4 + I_5 + (\frac{S_6}{V_5})^* + I_7 \tag{7}$$

The f_E function includes nonlinear correlation among state variables. As discussed in Section III, the function should be linearized first so that it can fit the linear state estimator.

In terms of S_6, (7) can be linearized as (8):

$$\begin{aligned} S_6 &= (\bar{I}_3^* - \bar{I}_4^* - \bar{I}_5^* - \bar{I}_7^*)V_5 \\ &\quad + \bar{V}_5(I_3^* - \bar{I}_3^*) - \bar{V}_5(I_4^* - \bar{I}_4^*) \\ &\quad - \bar{V}_5(I_5^* - \bar{I}_5^*) - \bar{V}_5(I_7^* - \bar{I}_7^*) \\ &= C_1 V_5 + C_2 I_3^* - C_2 I_4^* \\ &\quad - C_2 I_5^* - C_2 I_7^* + C_3 \end{aligned} \tag{8}$$

where $\bar{I}_3^*, \bar{I}_4^*, \bar{I}_5^*, \bar{I}_7^*$ is the mean of $I_3^*, I_4^*, I_5^*, I_7^*$ in the previous round of state estimation respectively and $I_i^* = I_{i,real} - jI_{i,imag}$.

C_1, C_2, C_3 can be calculated as (9)

$$\begin{cases} C_1 = \bar{I}_3^* - \bar{I}_4^* - \bar{I}_5^* - \bar{I}_7^* \\ C_2 = \bar{V}_5 \\ C_3 = -\bar{V}_5 \bar{I}_3^* + \bar{V}_5 \bar{I}_4^* + \bar{V}_5 \bar{I}_5^* + \bar{V}_5 \bar{I}_7^* \end{cases} \tag{9}$$

f_L describes the Ohm's Law on the conductor. The line impedance of the conductor is calculated with known line distance and conductor model specification. In Fig. 1, the f_L function at conductor 3 can be defined as (10):

$$V_4 - V_5 = I_3 * (R_3 + jX_3) \tag{10}$$

where $R_3 + jX_3$ is the line impedance of conductor 3.

In case of a basic ideal transformer, the factor function f_T can be defined as the following equations:

$$V_2 = V_1 t e^{j\theta} \tag{11}$$

$$V_2 I_2 = \rho V_1 I_1 \tag{12}$$

In (11), t is the turn ratio magnitude and θ is the phase shift angle. We use the simplified dc model for the step down transformer. Equation (12) is based on a dc converter with efficiency ρ. Ideally ρ equals 100%.

f_S and f_W define the correlation among solar and wind resources respectively. In the micro-grid state estimation, both the temporal and spatial correlations need to be considered. Extensive studies focus on the temporal correlation or the prediction of time series data from the REG (e.g. reference [11] and [12]). Since the cross correlation among neighboring sites may affect the total REG in a micro-grid, if the spatial correlation is not included in the factor function, the overall intermittence and variability of the REG may be underestimated.

In the linear state estimator, we need to define the linear correlation among multiple time series from the neighboring REG sites as the factor function. The spatio-temporal model that we propose consists of a vector autoregressive (VAR) specification, in comparison of the univariate autoregressive (AR) model for time series data from a single site. Reference [13]–[15] present similar approaches.

Suppose $X_{1,t}, X_{2,t}, ..., X_{k,t}$ are neighboring sites and their renewable generations are linearly correlated. The $k \times 1$ vector X_t represents the solar irradiance of site $1, 2, ..., k$ at time t.

$$X_t = \begin{pmatrix} X_{1,t} \\ X_{2,t} \\ ... \\ X_{k,t} \end{pmatrix} \tag{13}$$

The VAR model with prediction order p can be defined as (14):

$$X_t = c + \sum_{i=1}^{p} A_i X_{t-i} + \varepsilon_t \qquad (14)$$

where c is a constant and ε_t is the white noise. Matrix A_i and parameter ε_t can be derived by various VAR estimators (e.g. Levinson recursion, Burg-type Nuttal-Strand, etc. [16]). The correlation coefficient ρ between two solar/wind generation site i and j at the same time t satisfies:

$$\rho \propto e^{-\frac{d_{ij}}{L}} \qquad (15)$$

d_{ij} is the distance between site i and j. L is a scaling parameter related to weather condition [17]. It can be site specific or fixed within a geographic zonal area. For both cases, we can use training data to determine the parameter. In addition, previous studies show that the prediction model is not sensitive to the prediction order p, which means the spatio-temporal correlation can be described with the first order Markov process.

Due to the evolution of different weather types, the transition of different VAR models between successive regimes can describe the non-linearity of the time series REG data [18]. In terms of the solar irradiance time series, the cloud coverage of the sky is one factor of regime shifts. Reference [18]– [20] conduct experimental studies on the Markov Switching Vector Autoregressive (MS-VAR) Model.

V. STATE ESTIMATION

In the traditional power system state estimation, the voltages at all the buses are the variables to be estimated. The equations that involve real and reactive power should be nonlinear. In order to solve the nonlinear equations, the method of Newton Raphson [21] is applied and with the iterative algorithm the variables can converge to correct values. One commonly used iterative algorithm is the weighted least square (WLS) algorithm [22]. The algorithm can deal with multiple data sources with differing accuracy. In order to deal with the lack of measurements compared with unknown variables, pseudo-measurements are generated from historical load profile by different modeling techniques [23]. A minimum amount of measurements from metering devices are required in order to deliver true system state. The corresponding study is referred to as observability analysis.

In terms of micro-grid state estimation, currently many feeder circuits can barely provide any real-time measurements at the customer level. In order to fill the gap, we propose a new estimation algorithm (i.e. Belief Propagation (BP)), which has many applications in the communications and signal processing area [24][25]. The new technique can deal with sparse measurements based on the initialization of the states and refine the estimates with more incoming data. Furthermore, currently many researchers study the integration of the Advanced Metering Infrastructure (AMI) or Phasor Measurement Unit (PMU) data on the state estimation approach in order to increase the estimation accuracy. The high

resolution measurements can potentially increase the computation complexity of the centralized algorithm. In comparison, the BP computes local messages in a distributed manner and converges efficiently to the optimal estimates under many circuit configurations. The graphical model of the micro-grid captures the Markov property of the circuit topology that can be easily implemented with distributed algorithms such as the BP.

A. The BP algorithm

The BP algorithm is a message passing algorithm and is applied on graphical models. With proper definition of state variables and their correlations, the BP algorithm can be used for the purpose of real-time state estimation. At first we provide a reasonable set of initial probability distributions for all the variable nodes. The real-time model is built from the snapshots of real-time measurements. At certain time intervals, the computation center fetches data from the distributed metering devices. Given a new set of observations, the BP algorithm generates the global inference for every node based on current estimates.

When the graph is a tree, it is equivalent to the application of Gaussian elimination algorithm to derive the solution of a particular system of equations. In the spirit of the Kalman Filter algorithm [26], the inference can be derived in the following two steps within a rooted tree:

1) Fine-to-coarse Kalman filtering step, which is equivalent to Gaussian elimination.
2) Coarse-to-fine Kalman smoothing step or backsubstitution.

For the general non-rooted trees, the BP is equivalent to the Gaussian elimination in many-rooted trees. When the message is sent from node A to its neighboring node B, B is equivalently considered as the root of the graph [27]. This parallel message passing does not require specific schedule being calculated to ensure correctness of summation/integration. In every iteration the BP algorithm passes messages locally from variable nodes to their associate factor nodes and vice versa. After a certain number of iterations, all the messages converge to constant values. The global posterior inference can be calculated from the steady messages. The mathematical details of the BP algorithm can be found at [28] and [29]. Reference [9] lists the tabular computation rules for multivariate Gaussian BP.

The BP algorithm can converge to the true system states in the tree structure. When loops are included in the graph, the algorithm may oscillate and do not necessarily converge to the correct values. In our studies, most feeder circuits have radial structure, with a few exceptions addressing the back-up circuits. The factor function f_L and $f_{S/W}$ bring in new loops to the graphical model, as shown in Fig. 2. Empirical studies show that the BP algorithm can successfully converge to optimal estimates even in the loopy graph. Contingency analysis need to be conducted on the graph where the BP fails to converge. In these cases, additional observations should be

provided or certain loops that cause data conflicts need to be erased.

The BP algorithm is effective when the variable is discrete valued or continuous with Gaussian distribution. Here we adopt the assumption of Gaussian distribution and the algorithm is referred to as the Gaussian Belief Propagation (GaBP). In the GaBP algorithm, the messages only involve mean and variance, which avoids the calculation of pdf in the iterations. If the electrical parameters are Gaussian distributed, their entire pdf can be determined with the derived first and second order statistics. As discussed in Section III, Gaussian distribution can approximate the distribution of the state variables. However, without any assumption on the distribution of the state variables, as a maximum a posterior (MAP) approach the BP can deliver the linear minimum mean squared error estimation (LMMSE) of the true values. The LMMSE configuration should suffice the state estimation purpose. This justifies the application of GaBP solver in the micro-grid state estimator.

B. Measurements

The micro-grid state estimator should be provided with the following input [30]:

1) The bus/branch model of the micro-grid which includes lines, transformers, capacitors, sources, distributed generations and loads.
2) Component attributes.
3) Real-time voltage, real power and reactive power measurements at the substation, which typically come from SCADA.
4) Real-time feeder voltage and current measurements.
5) Real-time measurements at the operating nodes in the feeder circuits which are equipped with smart metering devices.
6) Distributed generation real and reactive power flow measurement.

The measurements can be sent to the local state estimator through the internet or power line communication. The convergence time of the BP algorithm depends on the network topology and the resolution of the observations. Although the data sampling rate can be quite high (determined by the metering devices), state estimation should run at the scanning rate which is subject to the communication delay and computational limitations.

Real-time measurements are provided from metering devices such as relay units, AMI and PMU. All these devices should be able to provide synchronized or time stamped data to facilitate dynamic system analysis. The measurements are subsampled and telemetered to the local energy control center on the micro-grid. For the part of the grid which does not require customer level granularity or does not have sufficient measurements to support reliable estimation, we can view that specific load zone as a single node and integrate all the downstream loads.

In the conventional DSE, the load is either a feeder circuit or the distribution system beyond the last substation. It is commonly modeled as constant power, current source or impedance. Real-time feeder measurements can be utilized to generate the constant load profile. In the micro-grid application, we use stochastic model of the load instead of constant load profile. In case of the lack of data, pseudo-measurements of time series data need to be generated. One approach is to scale down the zonal load to produce realistic time series load data on an individual distribution feeder [17]. In the future smart grid, the load should be demand responsive and in response to dynamic market prices. New load models which can address these new load characteristics will increase the accuracy of the model for the smart micro-grid.

VI. SIMULATION

The BP algorithm is simulated on the micro-grid model shown in Section II. The state variables and correlation functions for circuit components discussed in this paper are integrated into the simulation. Two extreme cases on the spatio correlation functions of the REG are tested and results are compared for the proof-of-concept study.

1) The REG sites are independent from each other.
2) The generation from REG sites within the feeder circuit is perfectly correlated (i.e. neighboring sites on the same feeder receive the same amount of solar irradiance).

	Independent (REG)		Perfect correlation (REG)	
	Round 1	Round 5	Round 1	Round 5
Iterations	4	2	6	2
Elapsed time(s)	0.0515	0.0136	0.0682	0.0226
Mean of difference from true values(|V|)	0.1932%	0.1952%	0.1932%	0.2077%

Fig. 5. Simulation results for the two extreme cases of renewable correlation

Matlab is used for the simulation. The program is run on a computer which has 3.2 GHz processor and 12 GB RAM. Fig. 5 compares the simulation results from the above two extreme cases of renewable correlation. The last row calculates $E[(\text{estimates - true values}) ./ \text{true values}]$ for the voltage magnitude. The left column reflects the results when we assume independent correlation. In every round, current estimates of the system states are utilized as the initialization and new set of observations are fetched to update the messages. In the first round, the initialization is set by the author. Using per unit value method, all the bus voltages are initialized to be $1p.u.$. Branch currents are chosen to satisfy the KCL. Intuitively, the convergence time of the following rounds should be less than the first round since the accuracy of initialization is refined after every round given reliable observations.

The right column shows the case of perfect correlation. Simulations show that the elapsed time for convergence is longer, since the REG correlation results in more loops and

the estimates oscillate around the correct values for a few iterations, as shown in Fig. 6 and Fig. 7.
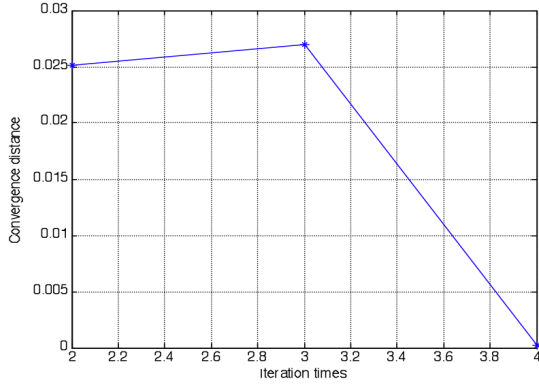

Fig. 6.   Convergence behavior for the case of independent correlation
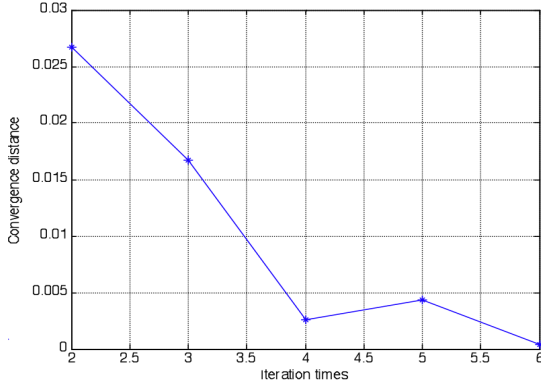

Fig. 7.   Convergence behavior for the case of perfect correlation

The y axis plots the values of the distance between estimates and true values. The algorithm can still converge to optimal values in the loopy graph, which is also shown from the percentage values of the error distances in the bottom row of Fig. 5.

As the initial simulation, the two extreme cases of renewable correlation can provide insights on the performance of the loopy BP. However, the two assumptions may oversimplify the realistic situation. Extensive studies/experiments need to be performed to validate the spatial-temporal model of the REG correlation discussed in Section IV. After the linear model is validated, the parameters for the linear correlation function can be derived for the sites of interest. We can then conduct new experiments on the calculated spatial-temporal model. For this purpose, the authors work closely with Hawaiian Electric Company, which provides us with island-wide environmental data from various solar and wind sensors. In addition, the information from weather stations would also benefit the study of regime shifts. Future research will utilize the validated correlation model to test the feeder circuits on the Oahu island.

VII. Conclusion

This paper presents a probabilistic approach of real-time state estimation which is different from any conventional state estimation method. It provides more accurate and timely information for monitoring and control purpose on the micro-grids while requiring real-time measurements from key locations of the system.

Future research includes continuing work on the model validation and the simulation studies. Spatio-temporal correlations for the REG as well as demand responsive models for customer loads are subject to the future study. The ability of the real time state estimation to predict and assess various failures on the micro-grid needs to be validated by both theoretical and simulation study. Last but not least, the optimal locations of deploying the smart metering devices can be a subsequent research based on the micro-grid state estimation result.

Acknowledgements

References

[1] A. Monticelli, "Electric Power System State Estimation", *Proceedings of the IEEE*, vol. 88, no. 2, Feb. 2000.

[2] H. Wang and N.N. Schulz, "A Revised Branch Current-Based Distribution System State Estimation Algorithm and Meter Placement Impact", *IEEE Trans. Power Syst.*, vol. 19, no. 1, Feb. 2004.

[3] A.P.S. Meliopoulos, G.J. Cokkinides, F. Galvan and B. Fardanesh, "Distributed State Estimator – Advances and Demonstration", *Proceedings of the 41st Hawaii International Conference on System Sciences*, pp. 163, Jan. 2008.

[4] U.S. Department of Energy, *The Smart Grid: An Introduction*.

[5] M. Baran and T.E. McDermott, "Distribution System State Estimation Using AMI Data", *Power Systems conference and Exposition, PSCE '09*, Apr. 2009.

[6] R. H. Lasseter, "Microgrids and Distributed Generation", *Journal of Energy Engineering, American Society of Civil Engineers*, Sep. 2007.

[7] G. D. Forney, Jr., "Codes on Graphs: Normal Realizations", *IEEE Trans. Inform. Theory*, vol. 47, no. 2, Feb. 2001.

[8] W. Hubbi and Y. Wang, "Effects of the Weighting Matrix on Power System State Estimation", *Electric Power Systems Research*, vol. 22, issue 1, pp. 35-39, Sep. 1991.

[9] H.-A. Loeliger, J. Dauwels, J. Hu, S. Korl, L. Ping and F. R. Kschischang, "The Factor Graph Approach to Model-Based Signal Processing", *Proceedings of the IEEE*, vol. 95, no. 6, Jun. 2007.

[10] R. Singh, B.C. Pal and R.A. Jabr, "Statistical Representation of Distribution System Loads using Gaussian Mixture Model", *IEEE Trans. Power Syst.*, vol. 25, no. 1, Feb. 2010.

[11] G. Papaefthymiou, P.H. Schavemaker, L. van der Sluis, W.L. Kling, D. Kurowicka and R.M. Cooke, "Integration of Stochastic Generation in Power Systems", *International Journal of Electrical Power and Energy Systems*, vol. 28, issue 9, pp. 655-667, Nov. 2006.

[12] P. Chen, T. Pedersen, B. Bak-Jensen, and Z. Chen, "ARIMA-Based Time Series Model of Stochastic Wind Power Generation", *IEEE Trans. on Power System*, DOI: 10.1109/TPWRS.2009.2033277.

[13] P. Chen, P. Siano, B. Bak-Jensen, and Z. Chen, "Stochastic Optimization of Wind Turbine Power Factor Using Stochastic Model of Wind Power", *IEEE Trans. on Sustainable Energy*, vol. 1, no. 1, Apr. 2010.

[14] X. De Luna and M.G. Genton, "Predictive Spatio-Temporal Models for Spatially Sparse Environmental Data", *Statistica Sinica*, vol. 15, pp. 547-568, 2005.

[15] C.A. Glasbey and D.J. Allcroft, "A Spatiotemporal Auto-regressive Moving Average Model For Solar Radiation", *Journal of the Royal Statistical Society: Series C (Applied Statistics)*, vol. 57, issue. 3, pp. 343-355, 2008.

[16] A. Schlogl, "A Comparison of Multivariate Autoregressive Estimators", *Signal Processing*, vol. 86, issue, 9, pp. 2426-2429, Sep. 2006.

[17] S. Kennedy, "Reliability Evaluation of Islanded Microgrids with Stochastic Distributed Generation", *Power & Energy Society General Meeting, IEEE*, pp. 1-8, Jul. 2009.

[18] P. Ailliot and V. Monbet, "Markov Switching Autoregressive Models For Wind Time Series", *Journal of Statistical Planning and Infererence*, Apr. 2006.

[19] C. Francq and J.-M. Zakoian, "Stationarity of Multivariate Markov-switching ARMA Models", *Journal of Econometrics*, pp. 339-364, 2001.

[20] Hans-Martin Krolzig, "Predicting Markov-Switching Vector Autoregressive Processes", *Journal of Forcasting*, Apr. 2000.

[21] J. Grainger and Jr. William Stevenson, "Power System Analysis", *McGraw-Hill Science/Engineering/Math*, ISBN-10: 0070612935, 1994.

[22] F.C. Schweppe and E.J. Handschin, "Static State Estimation In Electric Power Systems", *Proceedings of the IEEE*, vol. 62, pp. 972-982, July 1974.

[23] H. Wang and N.N. Schulz, "A Load Modeling Algorithm For Distribution System State Estimation", *Transmission and Distribution Conference and Exposition*, vol.1, pp. 120-105, 2001.

[24] Rusmevichientong, P.V. Roy, B., "An Analysis of Belief Propagation On the Turbo Decoding Graph With Gaussian Densities", *IEEE Trans. on Information Theory*, vol. 47, issue 2, pp. 745, Aug 2002.

[25] Hehn, T. Huber, J. Milenkovic, and O. Laendner, S., "Multiple-Bases Belief-Propagation Decoding of High-Density Cyclic Codes", *IEEE Trans. on Communications*, vol. 58, issue 1, pp. 1, Jan. 2010.

[26] G. Welch and G. Bishop, "An Introduction to The Kalman Filter", *UNC-Chapel Hill*, TR 95-041, Jul. 2006.

[27] K.H. Plarre, P.R. Kumar, "Extended Message Passing Algorithm for Inference In Loopy Gaussian Graphical Models", *Ad Hoc Networks*, vol. 2, issue. 2, pp. 153-169, Apr. 2004.

[28] M.I. Jordan, "Introduction to Probabilistic Graphical Models", unpublished, Nov. 2002

[29] F.R. Kschischang and B.J. Frey, "Factor Graphs and the Sum-Product Algorithm", *IEEE Trans. on Information Theory*, vol. 47, no. 2, Feb. 2001.

[30] R. Frowd, P. Parikh and B. Lawrence, "Real-Time Feeder Analysis and Control Using State Estimation", DTECH, 2010.